

Research

Specific wetting enthalpies for investigating lime surface properties due to the high temperature reactivity of limestone impurities

A. Lagazzo*, R. Botter and DT. Beruto

Department of Civil, Chemical and Environmental Engineering (DICCA), University of Genoa – Italy

***Corresponding author**

Alberto Lagazzo

Department of Civil
Chemical and Environmental
Engineering (DICCA)
University of Genoa
P.le J.F. Kennedy, pad. D, 16129
Genova, Italy
Tel. +390103536037
E-mail: alberto.lagazzo@unige.it

Received: September 12th, 2017

Accepted: September 19th, 2017

Published: September 25th, 2017

Citation

Lagazzo A, Botter R, Beruto DT. Specific wetting enthalpies for investigating lime surface properties due to the high temperature reactivity of limestone impurities. *Eng Press*. 2017; 1(1): 4-11. doi: 10.28964/EngPress-1-102

Copyright

©2017 Lagazzo A. This is an open access article distributed under the Creative Commons Attribution 4.0 International License (CC BY 4.0), which permits unrestricted use, distribution, and reproduction in any medium, provided the original work is properly cited.

ABSTRACT

In this paper, we address the role that limestone impurities play in the morphogenesis of different CaO-based particle surfaces. During the thermal decomposition of 00., such impurities can be the source of a complex pattern of reactions that form heterogeneous CaO-based surfaces. Our study reveals that this phenomenon is experimentally measurable once the level of impurities in the starting limestone is approximately 1.7% and the decomposition temperature is 1300°C. In limestones with impurity levels of 1% or less, the reactivity between them and the host CaO/CaCO₃ phases is reduced to a negligible level. To explore their average surface properties, we dispersed a set of heterogeneous lime powders in liquid paraffin and measured the correspondent exothermic wetting heat. Combining these results with Brunauer, Emmett and Teller (BET) measurements of the specific surface of the limes allows one to introduce a new parameter: the specific wetting enthalpy ξ (J/m²). Limes with nearly identical specific surface areas of approximately 1 m²/g can differ greatly in their ξ values, which range from -8 ± 0.2 J/m² to -1 ± 0.2 J/m². The specific wetting heats can be used as an intensive average thermodynamic parameter to characterise the chemical and physical properties of lime surfaces with specific surface energies that are experimentally undeterminable *via* calorimetric measurements.

KEY WORDS: CaO; Limestone; CaCO₃.

ABBREVIATIONS: BET: Brunauer, Emmett and Teller; SEM: Scanning Electron Microscope.

INTRODUCTION

CaO-based limes produced by decomposition of limestone can have different morphologies due to the presence of little amount of impurities in the CaCO₃. For some limes, powders are composed of a uniform set of grain aggregates similar to those generally observed.¹⁻⁴ After the decomposition of calcium carbonate powders in air. These morphologies can be associated with the solid-solid sintering process catalysed by the escaping CO₂.^{5,6} Sometimes, the edges of particles aggregates, where the particles have irregular shapes, tend to disappear and the external particle surface can be observed to have interesting patterns that resemble to Moire fringes.⁷ This is connected to the faceting mechanism and/or dissolution/recrystallization process of a low melting eutectic phase.⁸⁻¹¹ Thus, those findings indicate that limestone impurities strongly influence the physical and most likely the chemical properties of the obtained lime surfaces.¹² For many old and new technologies,¹³⁻²² lime is used for its surface properties, and there is a need to develop scientific knowledge in this complex and interesting field. Initially, evaluating the surface free energies of limes and the effect of lime impurities on these values seems to be a fairly reasonable way to proceed. Indeed, Brunauer, Kantro, Weise²³ and more recently, other researchers²⁴ have measured the heat of dissolution for oxides in the liquid phase (HNO₃, HCl and H₂O). Coupling these values with Brunauer, Emmett and Teller (BET) surface area measurements, they obtained acceptable

values for the specific surface enthalpies of these oxides. This value is similar to the specific surface free energy of the oxide neglecting entropy at room temperature. However, when the oxide is impure, as happens with limes, the surface enthalpy can be obscured by other bulk terms due to reactions between the impurities and the liquid phase. Therefore, it is impossible for this technique to determine the specific surface free energy of lime.

In two of our papers,^{25,26} we studied the dispersions of silica and kaolin powders in liquid paraffin containing aromatic and naphthenic compounds as a function of their concentration in the dispersed phase at 30 °C. The paraffin interacted with the solid surfaces to form thin solid-liquid interfaces and produced an exothermic wetting heat that accounted for the stability of the colloidal dispersion.²⁷ Theoretically, this mechanism involves three interactions: the van der Waals forces between solid particles, acid-base (Drago-Wayland)²⁸ attractive interactions between the silica and both the naphthenic paraffin and aromatic carbons, and repulsive steric interactions²⁹ between the layers adsorbed onto the silica surfaces. What matters to us is that non-bulk reactions occur between the liquid dispersant and the dispersed solid particles. Thus, for any given and selected liquid phase, the only information that can be derived from the measurable wetting heat relates to the nature of the dispersed solid particle surface. Whether the impurities are accessible to the lime surfaces or at the lime grain boundaries, their effect will change the corresponding exothermic wetting heat. This simple idea is the basis of the experimental method we use herein to obtain information on the surface impurities of lime and to gain insight into, as discussed below, how these impurities affect the morphogenesis of the CaO-based particles during the thermal decomposition of limestone. To the best of our knowledge, this

is a completely new approach to investigating lime surface properties and might be of interest to those who design lime particles with optimal properties for saving energy, adsorbing pollutants and other technological applications.³⁰⁻³⁴

EXPERIMENTAL

Materials

Limestones with a high calcium carbonate content ranging between 99.4 wt.% and 100 wt.%, are used to obtain the corresponding limes with CaO mol% ranging between 98.3 and 99.3. The chemical compositions of the limestones are reported in (Table 1). For all limestones, MgO is the primary impurity. LMST1 has a silica and alumina content greater than the other limestones.

Demineralised water and high purity liquid paraffin without the aromatic and naphthenic groups (0.88 g/cm³, boiling temperature of 68 °C, ignition point of 135 °C and viscosity of 20 mPas) were used as the liquid phase for the wetting experiments. The choose of this type of liquid paraffin is due to its high purity and to a degree of viscosity that allows a good dispersion of the lime powder inside the calorimetric cell.

Methods

Powder preparation: Limestone irregular blocks of 5-15 mm were decomposed in air for 2 h and 30 min at a constant temperature between 980 and 1300 °C according the samples producing limes with an average size between 1 and 8 μm. For some of these samples, a chemical analysis of the impurities was per-

	Limestone A	Limestone B	Lime A5	Lime B5
CaO	55.15	55.5	98.19	98.5
MgO	0.41	0.32	0.703	0.617
SiO ₂	0.24	0.05	0.322	0.051
Al ₂ O ₃	0.12	0.01	0.189	0.176
SrO	0.034	0.025	0.053	0.035
S	0.008	0.004	0.002	0.005
Fe ₂ O ₃	0.086	0.020	0.209	0.038
Na ₂ O	0.0083	0.0095		
MnO	0.0125	0.0081	0.0032	
P ₂ O ₅	0.0007	0.0084	0.003	0.0017
K ₂ O	0.0211	0.0019		
TiO ₂	0.0043	0.0059		
C org	0.03	0.03		
BaO	0.00052	0.00015		
V	0.00006	0.00007		
Zn	0.00012	0.0002		

Table 1: Main chemical components, in weight percentage, of limestone A and B of lime A5 and B5 obtained from decomposition at 1300 °C of the parent rock.

formed.

Reagent grade (r.g.) CaCO_3 powders were decomposed both at 900 °C for 30 min and 1350 °C for 4 hours to obtain small-surface CaO samples for comparison. All the CaO-based oxides were stored in sealed containers in a desiccator. Table 2 lists the lime families based on the limestone decomposition temperature and rock.

Calorimetric measurements: The enthalpy of hydration²³ and the heat of dispersion in liquid paraffin^{25,26} of the CaO-based oxides were evaluated through calorimetric analysis with a Setaram C80 calorimeter²⁵ equipped with stainless steel wetting cells. Two under vacuum closed glass ampoules of 5 mm in diameter, with a narrowing hook at one end to facilitate breaking, one filled with about 20 mg of lime powder sample and the other empty, were introduced into two identical cells (measure and reference respectively). The cells consisting in a cylinder of 2 cm in diameter and 10 cm in height, with a mobile piston inside, were then filled with 5 ml of liquid paraffin and then placed in the calorimetric at a temperature of 30 ± 0.01 °C. After the reaching of the thermal equilibrium (about 12 h), the piston was manually lowered to brake curved tip of the ampoule and the powders were wetted by the liquid phase. The heat flow was recorded until the flow curve reached the initial reference value, after about 12 h, suggesting that the reaction was completed. The use of an empty ampoule in the reference cell is necessary to remove the mechanical effects of the glass breaking and of the liquid entering in the glass container. All of the tests were repeated three times. The experimental error is contained under the 0.5%.

Nitrogen adsorption measurements at 78K: BET measurements were obtained with a symmetrical Sartorius microbalance described in detail previously.³³ The experimental error of the specific surface area was estimated to be approximately 3%.

Mercury porosimeter: Porosity and pore size distribution of the samples were analysed with a Thermo Scientific Pascal 240

mercury porosimeter equipped with a standard dilatometer for powders.

Scanning Electron Microscope (SEM): Morphological analyses of a carbon-coated sample were conducted using a scanning electron microscope (SEM) Hitachi-2500. The operating conditions were 20 kV.

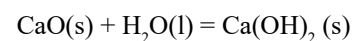
Theory of dissolution: It is known that the enthalpy of dissolution of a solid depends on its enthalpy of formation and on its surface area, whose contribute reduces the total amount of the heat developed during the dissolution.³⁵ In the case of the CaO dissolution, when the surface enthalpy is accounted for, any pure CaO sample with a given BET specific surface area will dissolve in liquid water with a global enthalpy change equal to:

$$-\Delta H_{\text{exp}} = -\Delta H_{\text{CaO,bulk}} + \sigma_{\text{CaO}} S_{\text{BET}} < 0$$

Where σ_{CaO} is the specific surface energy of the CaO and is always positive,³⁶ S_{BET} is the specific surface area of the CaO powders as evaluated using BET theory³⁷ and ΔH_{exp} and $\Delta H_{\text{CaO,bulk}}$ respectively the global experimental enthalpy of the CaO dissolution and the theoretical enthalpy of CaO dissolution. Thus, the dissolution of a CaO powder must yield an enthalpy change greater than that derived from the thermodynamic tables.

RESULTS AND DISCUSSION

CaO powders containing negligible impurities react with liquid water according to the general equation below:



The enthalpy change associated with reaction 1) can be derived from a selected thermodynamic table,³⁷ and has a value of -1160 J/g at 30°C.

Brunaer, Kantro and Weiss²³ conducted experiments with fine

Starting Limestone	Decomposition temperature [°C]	Obtained limes	Limes S_{BET} (m ² /g)
Limestone A	980	A1	2.8
	1060	A2	1.9
	1140	A3	1.2
	1200	A4	1.0
	1300	A5	0.7
Limestone B	980	B1	4.7
	1200	B4	1.2
	1300	B5	1
Powders of CaCO_3 R.G.	900	CaO 1 r.g.	11
	1350	CaO 5 r.g.	6.3

Table 2: List of starting limestones rocks decomposed at different temperature, in air, for 2.5 h, to obtain different set of limes with S_{BET} surface indicate in column 4.

and coarse CaO crystallites of 0.5 m²/g and of 7.8 m²/g, respectively, and found a consistent value for the CaO specific surface energy equal to 1310±200 mJ/m². No significant variations were observed if a 2N solution of HNO₃ was used instead of water. However, reproducing those experiments and obtaining coherent results when the specific surface area of the CaO reagents does not display significant differences is very arduous. We measured the surface energy of commercial grade CaO powders of 6 and 11 m²/g, and the results obtained of 1200±350 mJ/m² were affected by an experimental error too high lead to a CaO specific surface energy, which agrees well with Brunauer, Kanro and Weiss's data.

For this reasons the difference that can be attributed to the thermal effect due to the presence of the impurities is about equal to the experimental error of the calorimetric measure, that can be estimated to around 4%. Therefore, these difference in the global heats developed during the limes dissolution in water cannot be accounted to evaluate the quality and the micro-structural nature of the samples. In any case, also overcoming these experimental difficulties, the evaluation of the impurities through the effect that they produce on the enthalpy of CaO dissolution in water is cannot be calculated.

Considering a specific surface energy, σ_{Lime} , equal for all of the samples, then the plot standard heat of the dissolution reaction vs. surface area should form a straight line.²⁴ If this not occurs, reasonably can be conclude that the σ_{Lime} is different from lime to lime, even though they were obtained from the thermal decomposition of the same limestone parent.

In our previous paper,³⁹ we demonstrated that the lime grain surfaces can be quite heterogeneous due to the presence of limestone impurities. The derivation of $\sigma_{lime,i}$ values from a plot of $\Delta H_{lime,i,exp}$ vs. $S_{BET, lime,i}$ is a difficult task because of the following:

$$\sigma_{lime,i} = (\Delta H_{lime,i, bulk} - \Delta H_{lime,i, exp}) / S_{BET, lime,i}$$

If the impurities enter the bulk phase of the lime and react, then the state of the standard reference lime also changes. Thus, $\Delta H_{lime,i, bulk}$ is an unknown parameter. As a partial conclusion, any investigation into the surface properties of lime *via* the $\sigma_{lime,i}$ variable remains highly speculative and cannot be quantised from the experimental heat of reaction for lime powders dissolving in a liquid phase combined with the specific surface area measurements.

A kinetic approach, consisting in the measuring of parameter t_{60} , the time necessary in order that a CaO–water dispersion reaches the temperature of 60 °C, is well known and used in the industry.

The data of water reactivity tests (t_{60}) for limes obtained from different source of limestones (limestone A and limestone B), which have different amount of impurities is reported in (Figure 1). It is reasonable to assume that also the corresponding limes will have different amount of impurities, thus the comparison of their t_{60} values will give an idea of how the chemical impurities might influence the reactivity of the system lime-water. It is evident that limes with equal surface area, derived from limestones with greater amount of impurities, have a t_{60} parameter lower than the one for limes with less impurities. These data clearly prove that the degree of impurities in the limes does matter with its water reactivity.

It is interesting to discuss the evolution of the lime surface area as a function of the decomposition temperature of the parent limestone.

As reported in (Table 2), the specific surface area decreased as the decomposition temperature increased, however, the change

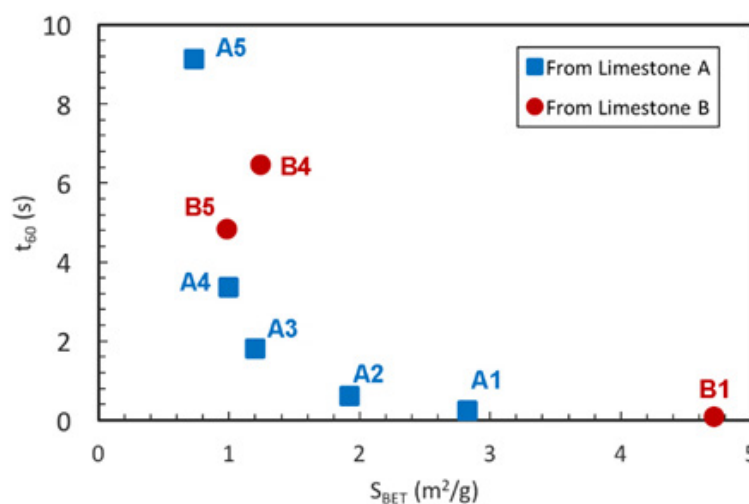


Figure 1: t_{60} for limes decomposed from limestone A and B against their specific surface area S_{BET}

is quite different between limes. For the sake of comparison, CaO (r.g.) was characterised by a surface area of 11 m²/g when the CaCO₃ was decomposed at 900 °C and 6 m²/g when kept for 4 hours at 1350 °C. These values are quite high relative to those obtained for the limes. Evidently, the impurities are an important variable in producing these effects. In particular limestone A decomposed at 980 °C produce lime with specific surface area of 2.8 m²/g while lime obtained at the same temperature from limestone B display a value of 4.8 m²/g. These experimental results support the hypothesis that limestone impurities are active at low temperatures where the catalytic action of the CO₂ on the densification of the CaO grains is the rate-determining step,⁴⁰ while others are more reactive at higher temperatures.

From the chemical analysis of the starting limestone, it can be observed that the molar fraction of the impurities covers only a narrow range. Thus, it is difficult to foresee which is the most effective for reducing the lime surface area.

To evaluate the surface reactivity of the limes samples, overcoming the difficulty connected with the calorimetric testes of CaO-based lime reacting with water, we describe the results obtained when the lime particles are dispersed in a liquid phase where the liquid molecules only adsorb onto the accessible lime surface. The dispersant liquid phase used herein is liquid paraffin, and the solid volume fraction, θ , of the dispersed lime particles was approximately 20 wt.%. This value can be considered greater than the percolate threshold.²⁹ Because the liquid paraffin does not contain aromatic and naphthenic groups, only two forces should be present: the attractive van der Waals forces and the steric repulsive forces between solid CaO particles and the adsorbed alkane molecules.

We introduce the variable ξ [J/m²], defined as:

$$\xi = \Delta H_w / S_{BET}$$

where ΔH_w [J/g] is the wetting heat of a given lime and S_{BET} is the associated specific surface area [m²/g]. This variable has been used in others paper^{25,41} and is strictly linked with the “quality” of the solid surface being investigated.

Figure 2 describes the parameter ξ vs. S_{BET} for the limes from limestone A and B. It can be observed that the points A are best-fitted by an equation that obeys the following phenomenological law:

$$\xi = -(\alpha S_{BET}) / (S_{BET} - \beta) \text{ [J/m}^2\text{]}$$

where α and β are the two best-fit constants for the lime/liquid paraffin system, which are equal to 0.43 and 0.675, respectively. It interesting to observe as the samples from limestone B do not follow the best-fit line.

ξ is an average intensive macroscopic parameter describing the capability of a lime surface to adsorb the liquid molecules and form the solid/liquid interface that make stable the dispersed solid powders. Thus, this variable depends on the accessibility of the internal surfaces (pores), external surfaces, and surface impurities to the liquid molecules, which can change the interactive forces between the solid surface and the liquid molecules.

The fact that sample A1 has a ξ value below that of lime A5 agrees with the morphological evidence (Figure 3), which supports the idea that limes with lower, but more accessible, surfaces can adhere more paraffin molecules per square metre than those with more surface area but smaller pores (Figure 4).

The grains of lime A1 (Figure 3a) can be describe as irregular polyhedral with an average dimension of 0.5-1 μm clustered in porous sintered aggregates similar to the one formed by the catalytic action of escaping CO₂. The grains of lime A5 (Figure 3b) have a different shape, and some are composed of large, flat surfaces with an average dimension of 20 μm × 0.2 μm .

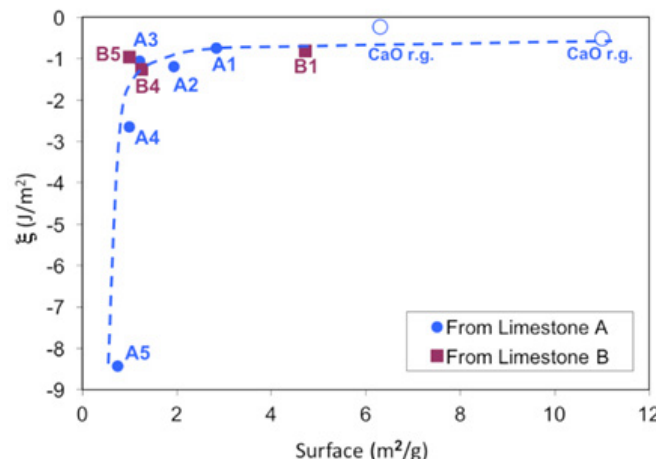


Figure 2: Specific wetting heat ξ of limes decomposed from limestone A, B and CaCO₃ r.g. against their specific surface area S_{BET}

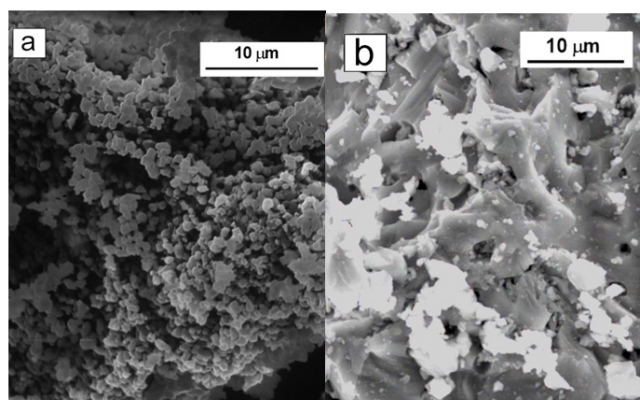


Figure 3: Morphological SEM image of lime A1 (a) and A5 (b) obtained for decomposition of limestone A at 980 °C and 1300 °C respectively.

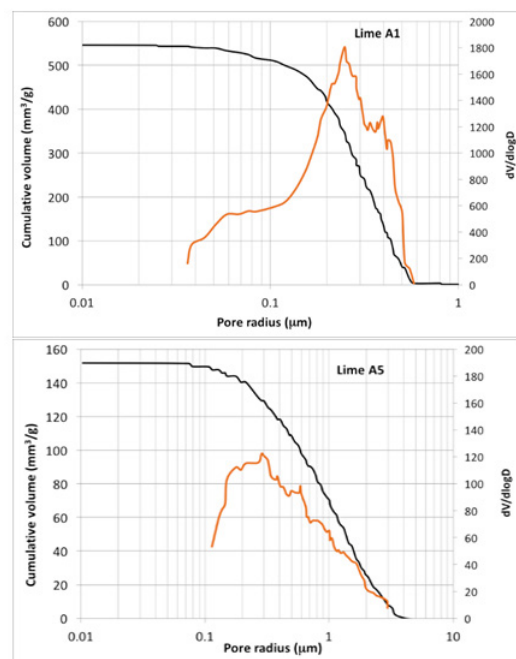


Figure 4: Cumulative and differential pore size distribution from Hg porosimeter analysis for sample A1 and A5.

The porosity and corresponding average pore size of sample A1 ($0.55 \text{ cm}^3/\text{g}$ and 0.4 nm , respectively) are higher than those for sample A5 ($0.15 \text{ cm}^3/\text{g}$ and 1 nm , respectively) and supports the inference from the SEM images in (Figure 3b).

However, morphological reasons alone are not enough to explain why the ξ values of limes from limestone A suddenly drop to -8 J/m^2 when the BET surface area is approximately $1 \text{ m}^2/\text{g}$, while for other limes from limestone B, the ξ values are fairly constant at approximately -1 J/m^2 even if the specific surface area is approximately $1.2 \text{ m}^2/\text{g}$.

In the author's opinion, this interesting datum depends on the content, nature and high-temperature reactivity of the limestone impurities.

Table 1 contains the chemical composition of lime A5 and B5 derived respectively from limestone A and B. It is evident that the impurity level in sample B5 is clearly lower than that of sample A5 with a containing of SiO_2 equal respectively to 0.051 wt.% and 0.322 wt.% and of Fe_2O_3 equal to 0.038 wt.% for B5 and 0.206 wt.% for A5. Thus, lime A5 has a ξ value of -8 J/m^2 not only because of its low S_{BET} surface area but also because the chemical active sites on its surface and the emerging grain boundaries are different from those for ξ values of approximately -1 J/m^2 . The high temperature reactivity of both the limestone impurities and the CaO and/or CaCO_3 phases in these rocks are most likely the explanation for this experimental evidence. In agreement with previous studies on the Al-SiO₂ system,³⁶ it has been shown that the aluminium ions can diffuse into NaCl-type oxides at the tetrahedral sites that form the AlO_4^- groups. Other studies⁸⁻¹¹ have proven the dramatic effects that adding impure

powders at higher concentrations has on the shape of the particles after the thermal decomposition of pure CaCO_3 powders.

When limes are obtained from limestone with impurities equal to or less than 1% that do not react during the decomposition of the parent limestone, the morphologies of the lime particles should be governed by the catalytic effect of escaping CO_2 , and the adsorption of the paraffin molecules would be primarily driven by the accessibility of the molecules to the lime surface.

CONCLUSIONS

In this paper, we analysed the role that limestone impurities have on the morphogenesis of different CaO-based particles. These impurities are a feature that geological history has left in the limestone. During the thermal decomposition of the parent limestone, these impurities can be the source of complex reaction patterns that lead to the morphogenesis of more heterogeneous aggregates of CaO-based grains. Our study reveals that decomposing limestones with 1.7% of impurities in air between 980 °C-1300 °C leads to lime grains with different shapes, while the limestones with impurities of 1% or less do not. In the latter case, the grain shapes look like those obtained from the decomposition of reagent grade CaCO_3 .

To explore the average surface energies of the heterogeneous lime particles, we have proposed dispersing the lime particles into a liquid vaseline and measuring their wetting heats. This parameter combines with the lime BET specific surface to create an important new parameter, ξ , which is the specific wetting heat of the dispersed powders. The plot of ξ vs. S_{BET} turns out to be a unique phenomenological rule for limes obtained from

all of the different sources. Based on the shape and value of ξ for each lime, it is possible to derive whether a scout molecule such as vaseline adsorbs under the action of weaker or stronger attractive forces. Stronger attractive fields were connected to the presence of surface active sites formed *via* high-temperature reactions between the limestone impurities and the CaO/CaCO₃ phase. These reactions are linked to the morphogenesis of the different sets of CaO-based particles, which are often observed from data concerning the structural and chemical analysis of lime.

CONFLICTS OF INTEREST

The authors declare that they have no conflicts of interest.

REFERENCES

1. Powell EK, Searcy AW. Surface-areas and morphologies of CaO produced by decomposition of large CaCO₃ crystal in vacuum. *J Am Cer Soc.* 1982; 65(3): c42-c44. doi: [10.1111/j.1151-2916.1982.tb10395.x](https://doi.org/10.1111/j.1151-2916.1982.tb10395.x)
2. Borgwardt RH. Calcination kinetics and surface area of dispersed limestone particles. *AIChE J.* 1985; 31(1): 103-110. doi: [10.1002/aic.690310112](https://doi.org/10.1002/aic.690310112)
3. Fuller EL, Yoos TR. Surface properties of limestones and their calcination products. *Langmuir.* 1987; 3: 753-760.
4. Beruto DT, Searcy AW, Kim MG. Microstructure, kinetic, thermodynamic analysis for calcite decomposition: Free surface and powder bed experiments. *Thermochimica Acta.* 2004; 424(1-2): 99-109. doi: [10.1016/j.tca.2004.05.027](https://doi.org/10.1016/j.tca.2004.05.027)
5. Erwing J, Beruto DT, Searcy AW. The nature of CaO produced by calcite powders decomposition in vacuum and in CO₂. *J Am Cer Soc.* 1979; 62(11-12): 580-84. doi: [10.1111/j.1151-2916.1979.tb12736.x](https://doi.org/10.1111/j.1151-2916.1979.tb12736.x)
6. Borgwardt RH. Calcium oxide sintering in atmosphere containing water and carbon dioxide. *Ind Engineering Chem Res.* 1989; 28(4): 493-500. doi: [10.1021/ie00088a019](https://doi.org/10.1021/ie00088a019)
7. Figueiredo M, Zerubia J, Jain AK. *Energy Minimization Methods in Computer Vision and Pattern Recognition.* Berlin, Germany: Springer; 2001.
8. Beruto DT, Searcy AW, Fulrath RM, Basu T. Effects of carbon dioxide and sodium chloride on the sintering of calcium oxide. *LBL.* 1977; 76: 101.
9. Beruto DT, Knudsen GF, Searcy AW. Effect of LiCl on the rate of calcite decomposition. *J Am Cer Soc.* 1982; 65(4): 219-22. doi: [10.1111/j.1151-2916.1982.tb10409.x](https://doi.org/10.1111/j.1151-2916.1982.tb10409.x)
10. Beruto DT, Barco L, Belleri G, Longo V. Interactions of LiBr with calcite and calcium oxide powders. *Cer Int.* 1983; 9(2): 53-58. doi: [10.1016/0272-8842\(83\)90023-8](https://doi.org/10.1016/0272-8842(83)90023-8)
11. Beruto DT, Kim MG, Barco L. Effect of Li₂CO₃ on the reaction between CaO and CO₂. *J Am Cer Soc.* 1984; 67(4): 274-278. doi: [10.1111/j.1151-2916.1984.tb18846.x](https://doi.org/10.1111/j.1151-2916.1984.tb18846.x)
12. Jing JY, Li TY, Zhang XW, et al. Enhanced CO₂ sorption performance of CaO/Ca₃Al₂O₆ sorbents and its sintering-resistance mechanism. *App Energy.* 2017; 199: 225-233. doi: [10.1016/j.apenergy.2017.03.131](https://doi.org/10.1016/j.apenergy.2017.03.131)
13. Boyton RS. *Chemistry and Technology of Lime and Limestone.* 2nd ed. New York, USA: Wiley-Interscience; 1980.
14. Konigsberger E, Konigsberger LG, Gamsjager H. *Geochim Cosmochim Acta.* 1999; 63(19-20): 3105-3119.
15. Salvador C, Lu D, Anthony EJ, Abanades JC. Enhancement of CaO for CO₂ capture in an FBC environment. *ChemEng J.* 2003; 96(1-3): 187-195. doi: [10.1016/j.ccej.2003.08.011](https://doi.org/10.1016/j.ccej.2003.08.011)
16. Lanás J, Alvarez JI. Dolomitic limes: Evolution of the slaking process under different conditions. *Thermochimica Acta.* 2004; 423(1-2): 1-12. doi: [10.1016/j.tca.2004.04.016](https://doi.org/10.1016/j.tca.2004.04.016)
17. Fennel PS, Davidson JF, Dennis JS, Hayhurst AN. Regeneration of sintered limestone sorbents for the sequestration of CO₂ from combustion and other systems. *J Energy Institute.* 2007; 80(2): 116-119.
18. Daniele V, Taglieri G, Quaresima R. The nanolimes in cultural heritage conservation: characterization and analysis of the carbonation process. *J Cult Heritage.* 2008; 9(3): 294-301.
19. Ströhle J, Galloy A, Epple B. Feasibility study on the carbonate looping process for post-combustion CO₂ capture from coal-fired power plants. *Energy Procedia.* 2009; 1(1): 1313-1320. doi: [10.1016/j.egypro.2009.01.172](https://doi.org/10.1016/j.egypro.2009.01.172)
20. Folger P. Carbon Capture: A technology assesment. Congressional Res Service 7-5700. 2013. Web site. <http://digitalcommons.unl.edu/crsdocs/19/>. Accessed September 11, 2017.
21. Skoufa Z, Antzara A, Heracleous E, Lemonidou AA. Evaluating the activity and stability of CaO-based sorbents for postcombustion CO₂ capture in fixed-bed reactor experiments. *Energy Procedia.* 2016; 86: 171-180. doi: [10.1016/j.egypro.2016.01.018](https://doi.org/10.1016/j.egypro.2016.01.018)
22. Granados-Pichardo A, Granados-Correa F, Sanchez-Mendieta V, Hernandez-Mendoza H. New CaO-based adsorbents prepared by solution combustion and high-energy ball-milling processes for CO₂ adsorption: Textural and structural influences. *Arabian J Chem.* 2017. Web site. <http://www.sciencedirect.com/science/article/pii/S1878535217300631>. Accessed March 21, 2017.

23. Brunauer S, Kantró DL, Weise CH. The surface energies of calcium oxide and calcium hydroxide. *Canadian J Chemistry*. 1956; 34(6): 729-742. doi: [10.1139/v56-096](https://doi.org/10.1139/v56-096)
24. Beruto DT, Rossi PF, Searcy AW. MgO of very high energy content from decomposition of $\text{Mg}(\text{OH})_2$. *J Phys Chem*. 1985; 89(9): 1695-1699. doi: [10.1021/j100255a031](https://doi.org/10.1021/j100255a031)
25. Beruto DT, Lagazzo A, Botter R. Silica–paraffin and kaolin–paraffin dispersions: Use of rheological and calorimetric methods to investigate the nature of their dispersed microstructure units. *Colloids Surface A*. 2012; 396: 153-160. doi: [10.1016/j.colsurfa.2011.12.062](https://doi.org/10.1016/j.colsurfa.2011.12.062)
26. Beruto DT, Lagazzo A, Botter R. Nanoscopic water layers adsorbed onto mesoporous silica aggregates and their effect on the stability and the static yield stress of their dispersion in liquid paraffin. *Colloids Surface A*. 2012; 407: 133-140. doi: [10.1016/j.colsurfa.2012.05.020](https://doi.org/10.1016/j.colsurfa.2012.05.020)
27. Dékány I. Microcalorimetric control of liquid sorption on hydrophilic/hydrophobic surfaces in nonaqueous dispersions. In: Dekker M, ed. *Thermal Behaviour of Dispersed Systems*. New York, USA: CRC Press; 2001.
28. Drago RS, Wayland BB. A Double–Scale Equation for Corre-ating Enthalpies of Lewis Acid–Base Interactions. *J Am Chem Soc*. 1965; 87(16): 3571-3577. doi: [10.1021/ja01094a008](https://doi.org/10.1021/ja01094a008)
29. Napper DH. *Polymeric Stabilization of Colloidal Dispersions*. New York, USA: Academic Press; 1983.
30. Abanades JC, Anthony EJ, Lu DY, Salvador C, Alvarez D. Capture of CO_2 from combustion gases in a fluidised bed of CaO. *AIChE J*. 2004; 50(7): 1614-1622. doi: [10.1002/aic.10132](https://doi.org/10.1002/aic.10132)
31. Hughes RW, Lu D, Anthony EJ, Yu Y. Improved long-term conversion of limestone-derived sorbents for in situ capture of CO_2 in a fluidized bed combustor. *IndEngChem Res*. 2004; 43(18): 5529-5539. doi: [10.1021/ie034260b](https://doi.org/10.1021/ie034260b)
32. Alvarez D, Abanades JC. Pore-size and shape effects on the recarbonation performance of calcium oxide submitted to repeated calcination/recarbonation cycles. *Energy & Fuels*. 2005; 19(1): 270-278. doi: [10.1021/ef049864m](https://doi.org/10.1021/ef049864m)
33. Husmann M, Zuber C, Maitz V, Kienberger T, Hochenauer C. Comparison of dolomite and lime as sorbents for in-situ H_2S removal with respect to gasification parameters in biomass gasification. *Fuel*. 2016; 181: 131-138. doi: [10.1016/j.fuel.2016.04.124](https://doi.org/10.1016/j.fuel.2016.04.124)
34. Beruto DT, Botter R, Searcy AW. H_2O catalyzed sintering of 2-nm-crosssection particles of MgO. *J Am Ceram Soc*. 1987; 70(3): 155-159. doi: [10.1111/j.1151-2916.1987.tb04950.x](https://doi.org/10.1111/j.1151-2916.1987.tb04950.x)
35. Costa GCC, Ushakov SV, Castro RHR, Navrotsky A, Mucillo R. Calorimetric measurement of surface and interface enthalpies of Yttria-stabilized Zirconia (YSZ). *Chem Mater*. 2010; 22(9): 2937-2945. doi: [10.1021/cm100255u](https://doi.org/10.1021/cm100255u)
36. Defay R, Prigogine I. *Surface tension and adsorption*. London: Longmans; 1966.
37. Brunauer S, Emmett PH, Teller E. Adsorption of Gases in Multimolecular Layers. *J Am Chem Soc*. 1938; 60(2): 309-319. doi: [10.1021/ja01269a023](https://doi.org/10.1021/ja01269a023)
38. The NBS tables of chemical thermodynamic properties. *J Phy Chem Ref Data*. 1982; 11(2).
39. Beruto DT, Botter R, Cabella R, Lagazzo A. A consecutive decomposition-sintering dilatometer method to study the effect of limestone impurities on lime microstructure and its water reactivity. *J European Cer Soc*. 2010; 30(6): 1277-1286. doi: [10.1016/j.jeurceramsoc.2009.12.012](https://doi.org/10.1016/j.jeurceramsoc.2009.12.012)
40. Busca G, Lorenzelli V. Infrared spectroscopic identification of species arising from reactive adsorption of carbon oxides on metal oxide surfaces. *Mater Chem*. 1982; 7(1): 89-126. doi: [10.1016/0390-6035\(82\)90059-1](https://doi.org/10.1016/0390-6035(82)90059-1)
41. Peng L, Qisui W, Xi L, Chaocan Z. The molar formation enthalpy of nano- SiO_2 with different surface area. *J Therm Anal Calorim*. 2009; 95(2): 667-670. doi: [10.1007/s10973-008-9325-3](https://doi.org/10.1007/s10973-008-9325-3)